Influence of Welding Thermal Cycles on Fatigue Fracture Behaviour of High-Strength Austenitic Steel

UDC:669.15-194.56:621.791
Original scientific paper https://doi.org/10.46793/adeletters.2026.5.2.4

Filip Klejch[1*], Eva Schmidova[1], Arman Dadkhah[1]

[1]Faculty of Transport Engineering, University of Pardubice, Pardubice, Czech Republic

Abstract:
This article investigates the fracture behaviour of high-manganese austenitic steel subjected to welding thermal cycles, with emphasis on welding-induced microstructural changes and their influence on fatigue performance. The aim of this research was to identify the mechanisms responsible for microstructural degradation caused by welding thermal cycles and to assess their effect on fatigue crack initiation and propagation. Combined metallographic and fractographic analyses were applied to two variants of high-strength austenitic steel: laser-deposited cast weld metal and a wrought profile developed for lightweight structural applications. The comparative analysis provides insight into how processing history and welding-induced microstructural changes influence fracture mechanisms, strain hardening, and fatigue crack growth in high-Mn austenitic steels.

ARTICLE HISTORY
Received: 6 April 2026
Revised: 5 June 2026
Accepted: 15 June 2026
Published: 22 June 2026

KEYWORDS
High-Mn austenitic steel,
High-strength steel,
Welding thermal cycle,
Fatigue crack propagation,
Strain hardening

1. INTRODUCTION

One of the current motivations for research on the mechanical behaviour of austenitic steels is applications in which component weight needs to be reduced while impact resistance needs to be improved [1, 2]. Maintaining good ductility with increased strength requires the development of new steel grades in which local strengthening mechanisms counteract the overall reduction in plasticity — and thus the energy required for fracture. This is achieved primarily by mechanisms such as dislocation hardening via twinning and martensitic transformation in response to dynamic loading [3, 4]. In addition to materials that are already widely used, particularly in the automotive industry, such as dual-phase and Transformation-Induced Plasticity (TRIP) steels, there is an ongoing development of materials in various modifications, such as medium-manganese steels and Twinning-Induced Plasticity (TWIP) steels [5-7]. Predicting the safety and service life of a specific application requires experimental analyses to quantitatively assess the degradation in the initial strength properties of the steel, as the induced processes cannot be reliably quantified by conventional materials testing methods [8].

Despite their promising mechanical performance, the potential of these advanced high-strength steels remains only partially exploited, not only because of their high production costs, but also because of the limited understanding of their structural behaviour. Computational models are being developed to support the design and optimisation of components made from these materials. The acceptance and reliability of these simulation tools depend on their ability to accurately reproduce experimental results, which is typically validated through sensitivity analyses and parametric studies [9-11].

A critical factor in the practical applicability of these materials is their response to the welding cycle, as the welding technique can significantly influence the degree of structural degradation of the steel [12-15]. Advanced high-strength austenitic steels are particularly sensitive to the thermal and, consequently, mechanical and strain cycles introduced during welding [16, 17]. The presented analyses demonstrate how welding

*CONTACT: Filip Klejch, e-mail: filip.klejch@upce.cz

induces structural changes in two representative high-strength austenitic steels, affecting their dynamic strength and fracture behaviour.

2. MATERIALS AND METHODS

This experimental study was focused on austenitic steels with increased manganese content (see Table 1), where variations in carbon content lead to the preference of different strengthening mechanisms:

- A wrought steel intended for application in safety components of welded structures made from profiles, specifically steel grade 1.4678.
- A weld deposit material in powder form intended for laser cladding - SZW 5049.

In material SZW 5049, the primary strengthening mechanism is deformation twinning, associated with a low stacking fault energy [18, 19], in contrast to steel 1.4678, which exhibits predominantly dislocation hardening and the formation of deformation bands. The influence of the applied heat results in different characteristics of structural degradation, with consequences for the deformation responses in relation to the design conditions of the structures (e.g. Eurocode 3, Part 1.4, and the design method based on deformation capacity).

Emphasis was placed on studying the changes in fracture mechanism and evolution under cyclic loading; selected results from metallographic and fractographic analyses of fatigue test specimens are presented. The planes for the metallographic cuts were oriented at the positions of fatigue crack initiation.

It should be noted that different types of samples were used depending on the specific application of the tested manganese austenitic high-strength steel variants. In the case of wrought profiles made from steel 1.4678, fatigue tests of butt welds (cross-section 3x25 mm) were performed; the weld deposit material was subjected to three-point cyclic bending of Charpy-type samples (cross-section 10x10 mm).

For material analyses, samples with no significant influence from welding defects were selected. The aim was to determine the critical material response to the welding cycle, focusing on the critical area of the weld joint and any potential impact of structural changes on the initiation of fatigue damage.

All analyses and tests were conducted at the Educational and Research Centre in Transport, University of Pardubice.

3. RESULTS AND DISCUSSION

For steel 1.4678, the local decrease in strength and the initiation of fatigue fracture were associated with the loss of initial dislocation hardening. Differences were also observed in the initial structural state of the steel, specifically variations in the homogeneity and intensity of dislocation hardening, the presence of heterogeneities and secondary phases. The initial microstructure with typical carbide rows in the austenitic matrix is shown in Fig. 1, while the heat-affected zone, the critical area in terms of thermal degradation of the steel, is shown in Fig. 2.

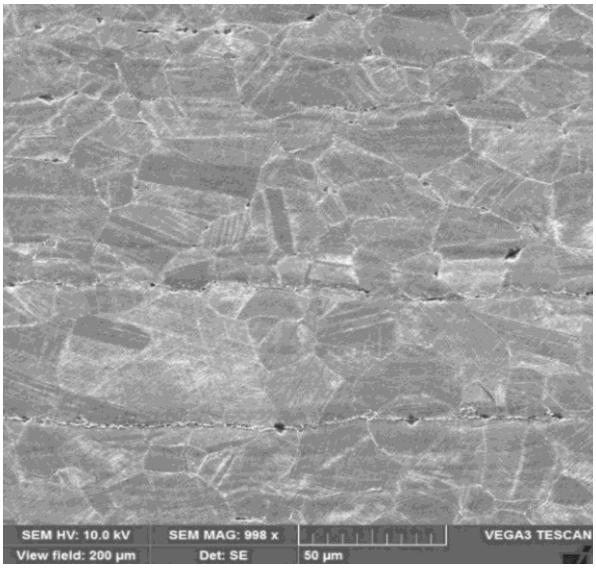

Fig. 1. Initial microstructure of steel 1.4678

Table 1. Chemical composition and mechanical parameters

Elements [wt. %]	C	Si	Mn	Cr	Cu	N	Ni	Mo	Cr	V
1.4678	0.31	0.39	15.91	14.01	0.50	0.33	-	-	-	-
SZW 5049	0.5	0.5	15	-	-	-	1	0.4	14	0.2
Mech. par.	**$Rp_{0.2}$ [MPa]**	**R_m [MPa]**	**A [%]**							
1.4678	811	1021	36							

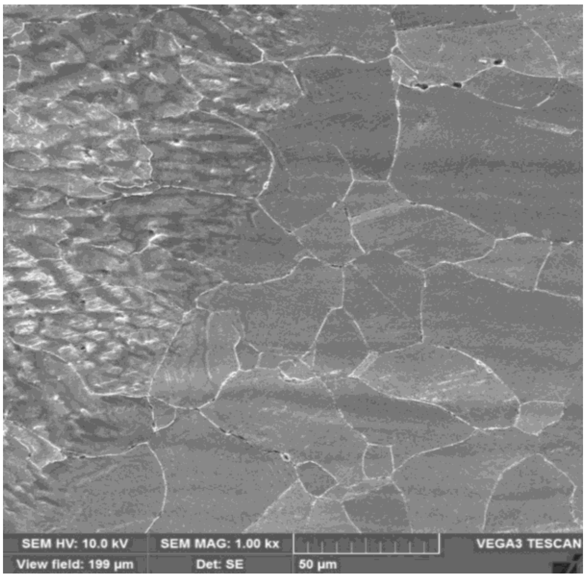

Fig. 2. Microstructure along the fusion zone - steel 1.4678

As a consequence of the welding process, discontinuous carbide precipitation was observed along the grain boundaries within the coarsened-grain region of the heat-affected zone. This microstructural evolution was accompanied by a reduction in dislocation-based strengthening, resulting from recovery processes activated by the welding thermal cycle. However, this effect extended only to a few tenths of a millimetre within the heat-affected zone.

The intensity of the structural changes along the weld interface arising from the combined effects of grain coarsening and a decrease in dislocation hardening is documented in Fig. 3. Fractographic analyses did not reveal any influence of the initial microstructural heterogeneities in the steel on failure initiation or propagation. However, their presence is reflected in local hardness variations outside the weld heat-affected zone, as shown in Fig. 4. The measured hardness gradient across the fusion zone at the fatigue crack initiation site indicates that the initial hardness reduction has only a minor structural impact.

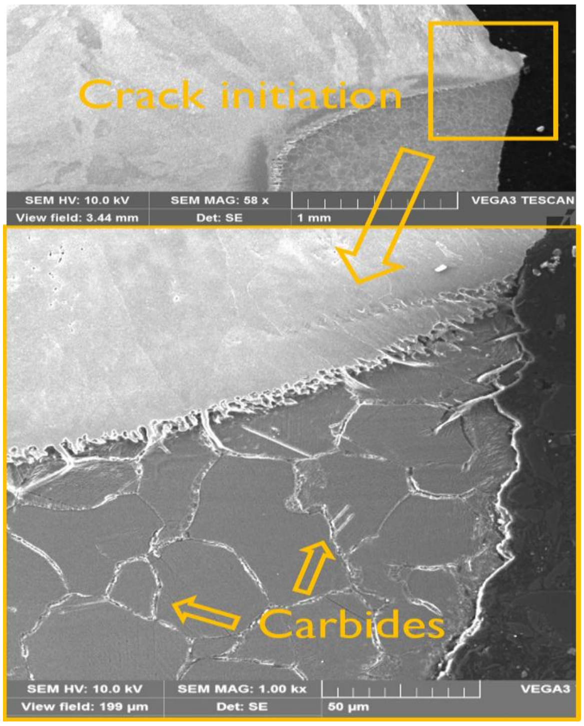

Fig. 3. Fatigue crack initiation

During fracture initiation and subsequent crack propagation, a localized increase in hardening was detected in the vicinity of the advancing crack tip. This partial “re-hardening” effect, attributed to intense local plastic deformation and renewed dislocation activity, is documented in Fig. 5. The phenomenon is associated with the accumulation of deformation-induced defects ahead of the crack tip, thereby increasing local material strength. Consequently, the localized re-hardening increases crack-tip resistance and reduces the driving force for crack advance, thereby slowing fatigue crack propagation [20, 21].

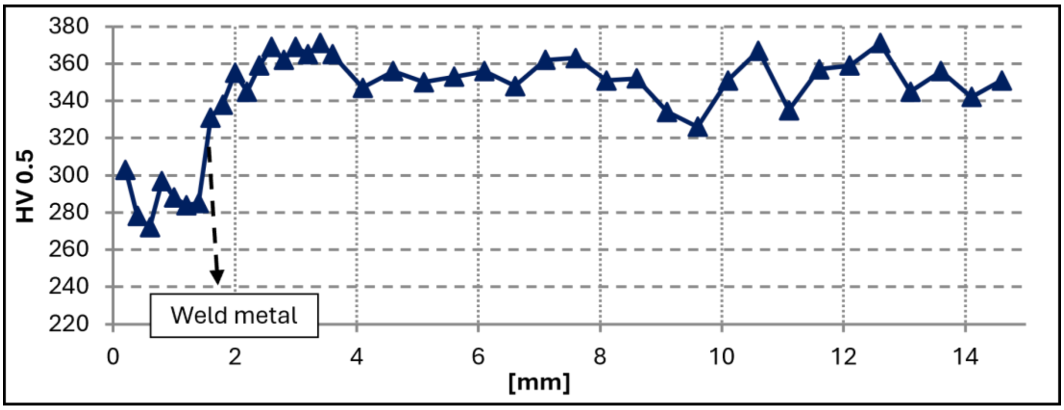

Fig. 4. Hardness profile across the weld joint in steel 1.4678

There is also a degree of material homogenisation that is observed within about 2 mm of the fusion boundary, reflecting limited microstructural recovery from welding.

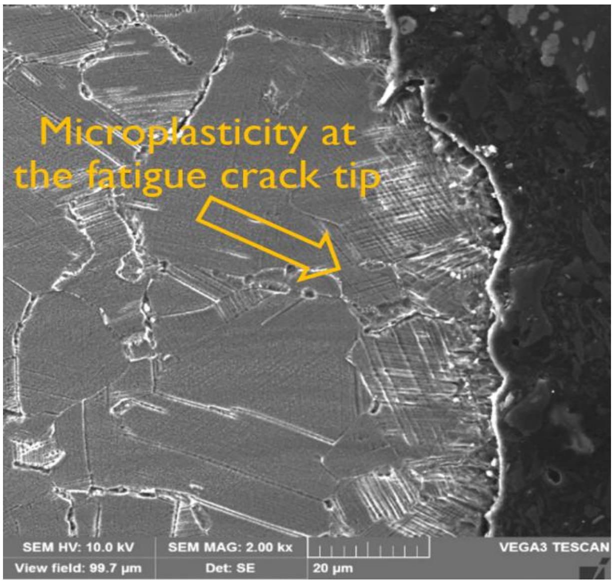

Fig. 5. Microplasticity at the fatigue crack tip

The fracture exhibited a partially crystalline appearance on the macroscopic scale (Fig. 6); therefore, the fracture surface in the area of initiation and primary crack propagation was further examined using microfractographic analysis.

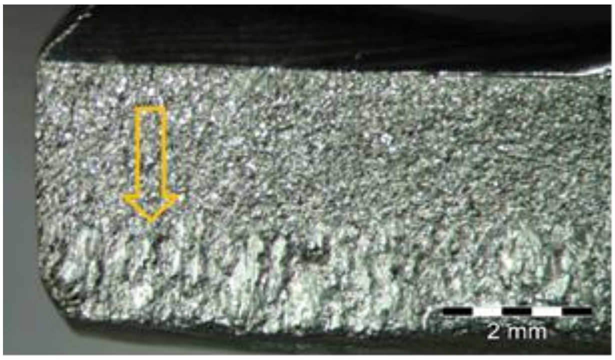

Fig. 6. Fracture surface with a crystalline appearance

Fractographic analysis was performed in correlation with metallographic examinations to obtain a comprehensive understanding of the microstructural factors influencing fracture behavior. Within the heat-affected zone (HAZ) of steel 1.4678, in addition to grain coarsening, partial carbide precipitation along grain boundaries was identified. Moreover, the observed reduction in dislocation density indicates diffusion-driven redistribution processes, particularly involving carbon, influencing local hardness and mechanical performance. To evaluate the potential impact of welding on the material's dynamic resistance, fatigue crack propagation was systematically compared between the as-received steel and butt-welded specimens produced using laser welding technology.

Fracture initiation occurred at the weld interface, indicating the effect of local stress concentrations in this region. To preserve the authenticity of the test and reflect realistic application conditions, the weld line was left unmodified/not ground. Microfractographic observations revealed the presence of cleavage facets in the initiation zone, while isolated cleavage facets were also detected within the region of primary fatigue crack propagation.

Fig. 7 illustrates the presence of transgranular cleavage fracture throughout the propagation stage across the HAZ. In evaluating the influence of structural modifications within the HAZ, it is important to note that no evidence of intergranular fracture was detected, indicating that the grain boundary did not play a significant role in crack propagation. The observed fracture morphology therefore reflects a localized reduction in ductility associated with the welding thermal cycle. Furthermore, the presence of cleavage facets during crack propagation in the as-received material indicates that strain hardening contributes to localized brittle features, highlighting the combined effects of cyclic loading and material hardening on fatigue crack growth in high-strength steels. These observations highlight the importance of microstructural control in the HAZ to ensure reliable performance of welded high-strength steels.

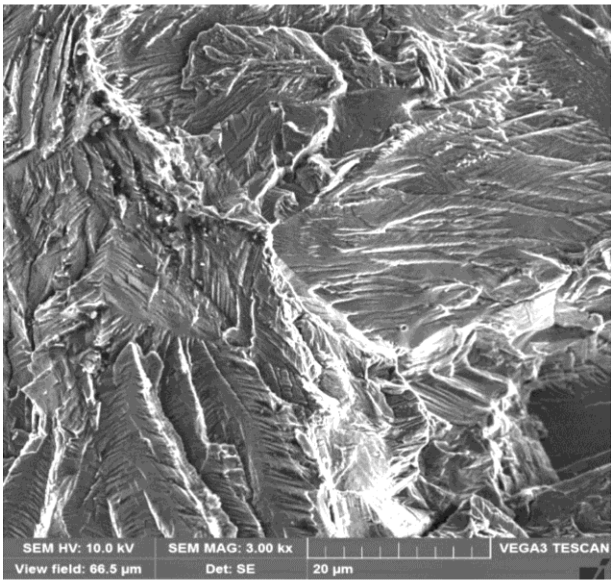

Fig. 7. Cleavage facets in the primary fatigue crack propagation zone

Fig. 8 illustrates the increase in crack growth rate as the fatigue crack propagates through the specimen. The final static fracture occurred via a predominantly ductile fracture mechanism, as shown in Fig. 9, with no anomalies or unexpected fracture features observed.

Although banded microstructural heterogeneity was present in the central region of the cross-section, it did not contribute to fracture initiation, indicating that these inherent variations in microstructure did not affect the material's fatigue resistance. Locally induced delamination was observed only during the final fracture stage and was confined to small regions, with no significant effect on fatigue life. These results highlight the dominant role of the weld interface and HAZ in crack initiation and propagation, while the bulk material heterogeneities had a negligible effect on fatigue performance.

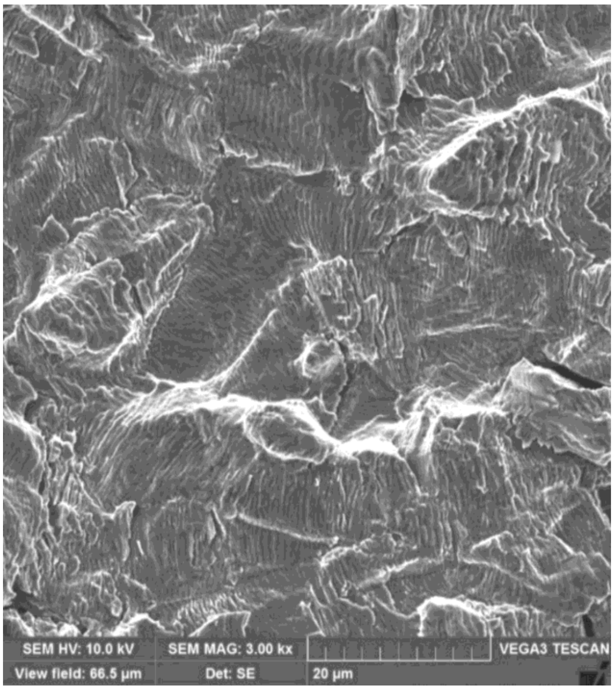

Fig. 8. Fatigue crack propagation close to unstable crack growth

In the case of laser cladding (material SZW 5049), the analysis focused not only on the effects of repeated thermal cycling associated with cladding layers but also on the potential for diffusion-controlled carbon redistribution at the clad–substrate interface, with potential implications for local microstructural evolution and mechanical response.

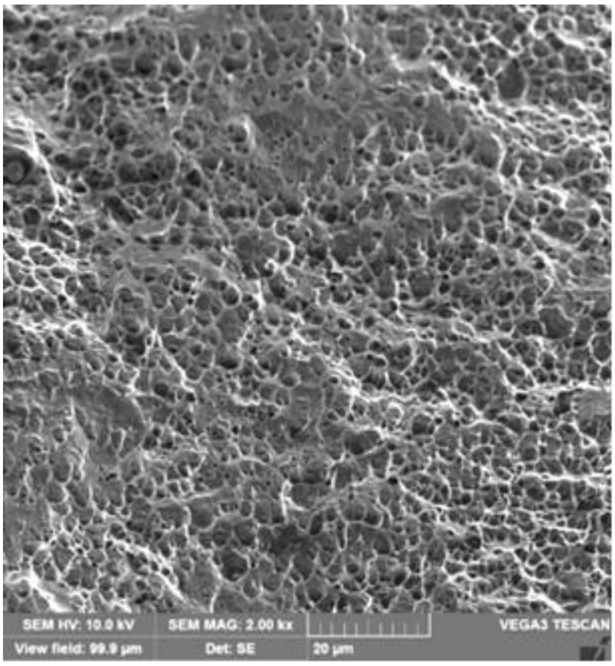

Fig. 9. Static ductile fracture

In this case, the base material was a pearlitic steel with a carbon content close to the eutectoid composition. The laser cladding process resulted in negligible dilution of the deposited material, while decarburization of the pearlitic substrate was restricted to a narrow region limited to less than 0.05 mm from the fusion boundary, as shown in Fig. 10. Detailed microstructural characterization revealed carbide precipitation along austenitic grain boundaries in the vicinity of the fusion zone; however, both the extent and morphology of these carbides were comparable to those observed in the upper cladding layers. These upper layers were identified as the critical regions for fatigue crack initiation under the applied loading conditions. Despite the significant presence of non-metallic inclusions within the weld metal, fractographic observations indicated that these features did not play a dominant role in fatigue crack propagation, as illustrated in Fig. 11.

Similar to the previously investigated high-strength austenitic steel, cleavage-type fracture was observed in the crack initiation region and during the early stages of fatigue crack propagation. The occurrence of these fracture characteristics indicates a localized reduction in ductility associated with intense plastic deformation in the vicinity of the crack tip. In both materials, the results demonstrate a pronounced contribution of strain-hardening mechanisms during the initial stages of the fatigue process, which locally modify the stress–strain response and influence the early evolution of fatigue damage and crack growth behaviour.

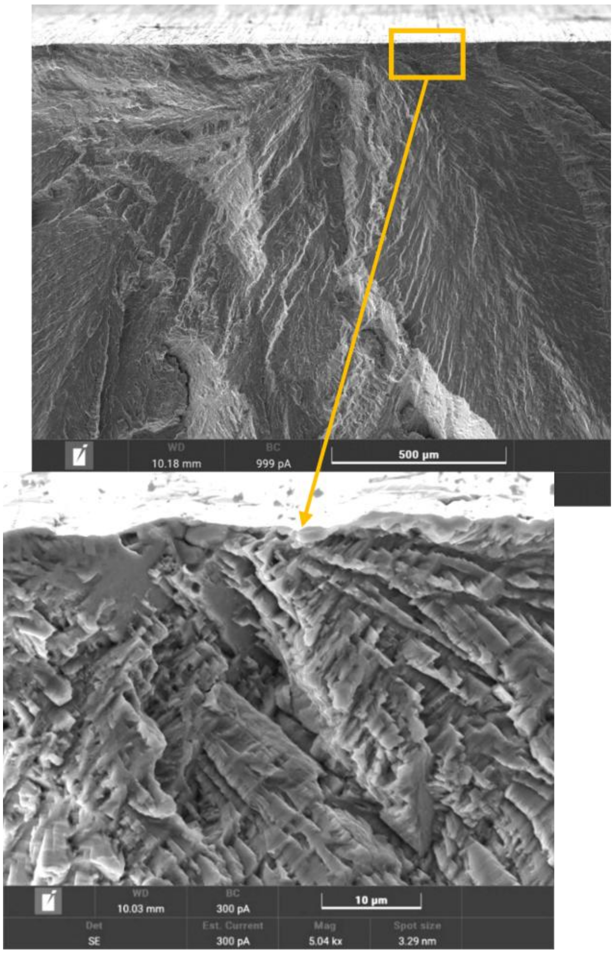

Fig. 10. Fusion zone of laser cladded material

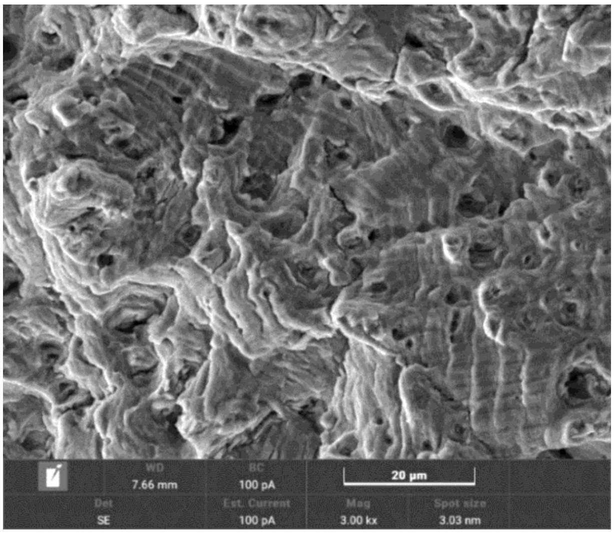

Fig. 11. Fatigue crack propagation

4. CONCLUSIONS

This study was focused on the specific response of high-strength austenitic manganese steels to cyclic loading, with particular emphasis on weld-induced microstructural degradation and its influence on fatigue performance. The same fatigue crack propagation mechanism was identified in both analyzed material variants—the laser-deposited weld metal and the wrought profile designed for lightweight structural applications—indicating comparable crack growth behaviour. A key finding is the occurrence of continuous strain hardening driven by microplastic deformation in the vicinity of the advancing fatigue crack tip, which locally modifies the stress–strain response and plays a significant role in fatigue crack propagation under cyclic loading conditions.

The specific morphology of the fatigue fracture was driven by localized deformation at grain boundaries, particularly in regions where slip bands intersected along different slip systems. Such interactions promote the separate initiation of microcracks and fundamentally influence the resulting fracture path. The fatigue behaviour of both analysed steel types was found to be strongly dependent on strain-hardening mechanisms, with fatigue crack nucleation occurring preferentially at intersections of slip bands or deformation twins. Fatigue tests on similar steels reported in the literature (e.g., [22]) confirm that crack initiation typically takes place at an early stage of cyclic loading, before 25% of the total fatigue life. The subsequent rapid propagation and coalescence of microcracks along grain boundaries indicate an inherent grain-boundary weakness, which is typical of high-Mn austenitic steels. As a consequence, the fracture surface often exhibits mixed-mode characteristics, transitioning to quasi-cleavage during the final fracture stage. However, in the present analyses, crack propagation was found to occur along slip lines or twins, resulting in an overall transgranular fracture mode.

From the perspective of welding-induced effects, a key observation is that the contribution of cleavage-type fracture, occasionally detected even during the initiation and early propagation stages of the fatigue crack, is not directly attributable to microstructural degradation of the steel, such as the carbon redistribution or carbide precipitation along slip planes or grain boundaries expected. Instead, the degree of observed cyclic hardening was found to be strongly dependent on grain size, which represents the main microstructural parameter influenced by the welding thermal cycle. The performed analysis shows that the damage evolution associated with cyclic loading actively contributes to work hardening, increasing local crack-tip resistance and effectively stabilizing the fatigue crack propagation process.

ACKNOWLEDGEMENT

This study has been accomplished with the support of the University of Pardubice under project no. SGS_2026_009 and project no. TC510177. The authors gratefully acknowledge the support provided by these projects.

CONFLICTS OF INTEREST

The authors declare no conflict of interest.

REFERENCES

[1] C. Scott, S. Allain, M. Faral, N. Guelton, The development of a new Fe-Mn-C austenitic steel for automotive applications. *Revue de Métallurgie*, 103(6), 2006: 293-302. https://doi.org/10.1051/metal:2006142

[2] G. Frommeyer, U. Brüx, P. Neumann, Supra-ductile and high-strength manganese-TRIP/TWIP steels for high energy absorption purposes. *ISIJ International*, 43(3), 2003: 438-446. https://doi.org/10.2355/isijinternational.43.438

[3] M. Eskandari, M.A. Mohtadi-Bonab, M. Yeganeh, J.A. Szpunar, A.G. Odeshi, High-strain-rate deformation behaviour of new high-Mn austenitic steel during impact shock-loading. *Materials Science and Technology*, 35(1), 2019: 77-88. https://doi.org/10.1080/02670836.2018.1540507

[4] L.A. Dobranski, W. Borek, J. Mazurkiewicz, Mechanical properties of high-Mn austenitic steel tested under static and dynamic conditions. *Archives of Metallurgy and Materials*, 61(2), 2016: 725-730. https://doi.org/10.1515/amm-2016-0124

[5] B.C. De Cooman, Y. Estrin, S.K. Kim, Twinning-induced plasticity (TWIP) steels. *Acta Materialia*, 142, 2018: 283-362. https://doi.org/10.1016/j.actamat.2017.06.046

[6] Y.-K Lee, J. Han, Current opinion in medium manganese steel. *Materials Science and Technology*, 31(7), 2015: 843-856. https://doi.org/10.1179/1743284714Y.0000000722

[7] O. Grässel, L. Krüger, G. Frommeyer, L.W. Meyer, High strength Fe–Mn–(Al, Si) TRIP/TWIP steels development—properties—application. *International Journal of Plasticity*, 16(10-11), 2000: 1391-1409. https://doi.org/10.1016/S0749-6419(00)00015-2

[8] J. Lemaitre, R. Desmorat, Engineering damage mechanics: Ductile, creep, fatigue and brittle failures. *Springer Berlin Heidelberg*, 2005. https://doi.org/10.1007/b138882

[9] S. Allain, J.-P. Chateau, O. Bouaziz, A physical model of the twinning-induced plasticity effect in a high manganese austenitic steel. *Materials Science and Engineering: A*, 387-389, 2004: 143-147. https://doi.org/10.1016/j.msea.2004.01.060

[10] J. Neuhäusler, J. Roth, M. Oswald, A. Dürr, K. Rother, Sequence effects on the life estimation of thin-walled welded tubular structures made of HSS + UHSS under bending. *Welding in the World,* 67(3), 2023: 683–705. https://doi.org/10.1007/s40194-022-01432-z

[11] J. Neuhäusler, J. Roth, M. Oswald, A. Dürr, K. Rother, Sequence effects on the life estimation of welded tubular structures made of S355J2H under uniaxial fatigue loading. *Welding in the World*, 68(5), 2024: 1103-1141. https://doi.org/10.1007/s40194-023-01605-4

[12] K. Wang, T. Bai, J. Xu, Q. Ma, P. Wang, R. Chen, L. Li, Surface treatment of rail to enhance rolling contact fatigue and wear resistance: Combined spot laminar plasma quenching and tempering method. *Construction and Building Materials*, 401, 2023: 132832. https://doi.org/10.1016/j.conbuildmat.2023.132832

[13] M. Dahmen, S. Lindner, D. Monford, D. Petring, Weld metallurgy and mechanical properties of high manganese ultra-high strength steel dissimilar welds. *Physics Procedia*, 83, 2016: 344-351. https://doi.org/10.1016/j.phpro.2016.08.036

[14] L. Mujica, S. Weber, C. Thomy, F. Vollertsen, Microstructure and mechanical properties of laser welded austenitic high manganese steels. *Science and Technology of Welding and Joining,* 14(6), 2009: 517-522. https://doi.org/10.1179/136217109X434243

[15] G. Park, S. Jeong, C. Lee, Fusion weldabilities of advanced high manganese steels: A review. *Metals and Materials International*, 27(7), 2021: 2046-2058. https://doi.org/10.1007/s12540-020-00706-9

[16] I. Mejía, H. Hernández-Belmondez, C. Maldonado, Weldability of High-Mn Austenitic Twinning-Induced Plasticity (TWIP) Steel Microalloyed with Nb. *MRS Advances*, 2(62), 2017: 3899-3908. https://doi.org/10.1557/adv.2018.108

[17] M.M.Z. Ahmed, E. Ahmed, A.S. Hamada, A.S. Khodir, M.M. El-Sayed Seleman, B.P. Wynne, Microstructure and mechanical properties evolution of friction stir spot welded high-Mn twinning-induced plasticity steel. *Materials & Design*, 91, 2016: 378-387. https://doi.org/10.1016/j.matdes.2015.12.001

[18] E. Bayraktar, F.A. Khalid, C. Levaillant, Deformation and fracture behaviour of high manganese austenitic steel. *Journal of Materials Processing Technology*, 147(2), 2004: 145-154. https://doi.org/10.1016/j.jmatprotec.2003.10.007

[19] M. Dahmen, B. Deniz, D. Petring, Revisiting transport phenomena and their role in intermixing during dissimilar laser beam welding. *Procedia CIRP*, 94, 2020: 726-730. https://doi.org/10.1016/j.procir.2020.09.132

[20] P. Gallo, P. Lehto, E. Malitckii, H. Remes, Influence of microstructural deformation mechanisms and shear strain localisations on small fatigue crack growth in ferritic stainless steel. *International Journal of Fatigue*, 163, 2022: 107024. https://doi.org/10.1016/j.ijfatigue.2022.107024

[21] T. Niendorf, F. Rubitschek, H.J. Maier, J. Niendorf, H.A. Richard, A. Frehn, Fatigue crack growth—Microstructure relationships in a high-manganese austenitic TWIP steel. *Materials Science and Engineering: A*, 527(9), 2010: 2412-2417. https://doi.org/10.1016/j.msea.2009.12.012

[22] A.S. Hamada, L.P. Karjalainen, J. Puustinen, Fatigue behavior of high-Mn TWIP steels. *Materials Science and Engineering: A*, 517(1-2), 2009: 68-77. https://doi.org/10.1016/j.msea.2009.03.039